ChemPubSoc Europe

DOI: 10.1002/cphc.201600063

CHEMPHYSCHEM Articles

Structures of Trichloromethyl Thiocyanate, CCl_3SCN, in Gaseous and Crystalline State

Yanina Berrueta Martínez,[a] Lucas S. Rodríguez Pirani,[a] Mauricio F. Erben,[a] Roland Boese,[b] Christian G. Reuter,[c] Yury V. Vishnevskiy,[c] Norbert W. Mitzel,*[c] and Carlos O. Della Védova*[a]

Trichloromethyl thiocyanate, CCl_3SCN, was structurally studied in both the gas and crystal phases by means of gas electron diffraction (GED) and single-crystal X-ray diffraction (XRD), respectively. Both experimental studies and quantum chemical calculations indicate a staggered orientation of the CCl_3 group relative to the SCN group. This conclusion is supported by the similarity of the C–SCN bond length to that of the *anti*-structure of CH_2ClSCN (Berrueta Martínez et al. *Phys. Chem. Chem. Phys.* 2015, *17*, 15805–15812).[1] Bond lengths and angles are similar for gas and crystal CCl_3SCN structures; however, the crystal structure presents different intermolecular interactions. These include halogen and chalcogen type interactions, the geometry of which was studied. Characteristic C-Y···N angles (Y = Cl or S) close to 180° provide evidence for typical σ-hole interactions along the halogen/chalcogen–carbon bond in N···Cl and N···S, intermolecular units.

1. Introduction

Trichloromethyl thiocyanate, CCl_3SCN, has been the object of a range of studies, and the use of thiocyanate species as a control agent against insect pests has been proposed.[2,3] Moreover, experimental IR and Raman spectroscopic data as well as theoretical investigations on this compound have been reported.[4]

A range of technological applications, including crystal engineering and the development of new pharmaceutical compounds rely on the knowledge of intermolecular interactions.[5] Chalcogen and halogen intermolecular interactions have become the focus of many investigations, especially on bimolecular complexes.[6] In the case of CCl_3SCN, both chalcogen and halogen intermolecular contacts are possible in the crystal phase. The nitrogen atom of the title compound is likely to participate in both halogen (with chlorine) and chalcogen (with sulfur) interactions. However, structural studies in different phases are not often presented together in the literature. In this sense, the effects of intermolecular interactions in the solid state are not always discovered and analyzed. We intended to study intermolecular interactions in crystals of CCl_3SCN. To evaluate the effect of intermolecular interactions on the molecular bonding we also studied the structure of the free molecule in the gas phase. Studies and a characterization of the intermolecular bonding by geometrical criteria are reported within this contribution.

[a] *Y. Berrueta Martínez, Dr. L. S. Rodríguez Pirani, Dr. M. F. Erben, Dr. C. O. Della Védova*
CEQUINOR (CONICET-UNLP), Departamento de Química
Facultad de Ciencias Exactas, Universidad Nacional de La Plata
47 esq. 115, 1900 La Plata (Argentina)
E-mail: carlosdv@quimica.unlp.edu.ar

[b] *Dr. R. Boese*
Strukturchemie, Institut für Anorganische Chemie
Universität Duisburg Essen, Universitätsstraße 7
45117 Essen (Germany)

[c] *C. G. Reuter, Dr. Y. V. Vishnevskiy, Dr. N. W. Mitzel*
Lehrstuhl für Anorganische Chemie und Strukturchemie
Centre for Molecular Materials CM2, Universität Bielefeld
Universitätsstraße 25, 33615 Bielefeld (Germany)
E-mail: mitzel@uni-bielefeld.de

Supporting Information and the ORCID identification number(s) for the author(s) of this article can be found under http://dx.doi.org/10.1002/cphc.201600063.

2. Results and Discussion

2.1. Computational Chemistry

The potential function for the rotation around the φ(Cl-C-S-C) dihedral angle was calculated for CCl_3SCN by using the B3LYP/cc-pVTZ and MP2/cc-pVTZ levels of theory, for which the expected symmetric curve with minima at 60° was observed (Figure 1). Maxima in the potential energy curves were ob-

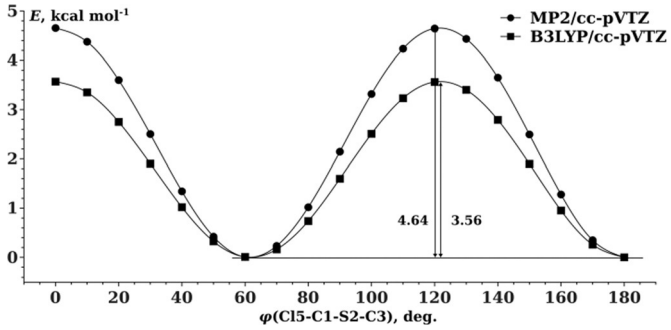

Figure 1. Potential energy functions of the internal rotation about the C1–S2 bond of CCl_3SCN.

served for structures with eclipsed orientation between the halo-methyl and the SCN groups. Qualitative agreement was obtained between the two quantum-chemical methods used here. The B3LYP level, however, predicted lower energy barriers than the MP2 method. At the second stage of the theoretical analysis, the geometry corresponding to the minimum was fully optimized (Figure 2) with subsequent frequency calculations at the same levels of theory.

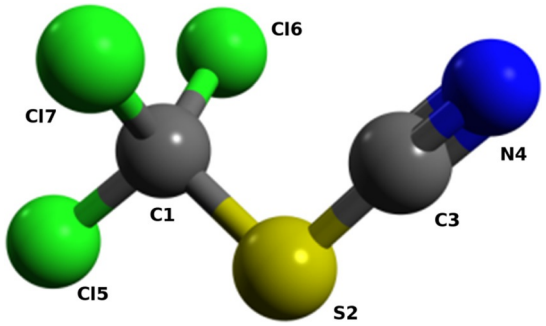

Figure 2. Molecular structure and atom numbering scheme of CCl_3SCN.

We used four different methods, DFT (B3LYP), MP2, CCSD, and CCSD(T) with cc-VTZ basis sets, to compute the dependence of the predicted structure on the level of calculation. As expected, the values calculated by DFT (B3LYP) systematically differ from those of the three other methods. Among the bond lengths, the largest difference between B3LYP and MP2 predictions is 0.028 Å for C1–S2 bonds. Interestingly, the length of the triple C≡N bond predicted by B3LYP (1.156 Å) is very close to that of the CCSD calculations (1.155 Å). The structural results of these calculations are presented in comparison with the experimental parameters obtained by means of XRD and GED in the next section (Table 1).

We also tested the CCSD method and the high-level CCSD(T) of approximation to evaluate the improvement upon inclusion of perturbed triple corrections in the coupled-cluster scheme. When switching from CCSD to CCSD(T) level of theory, most bond lengths were found to increase by 0.005–0.009 Å in length, with the exception of the bond S2–C3. The most significant change was observed for the triple bond C≡N (from 1.155 to 1.164 Å). In contrast, the angles were predicted to be nearly the same in both calculations, with a maximum difference of 0.2°.

2.2. Molecular Structures in the Gas Phase

An experimental determination of the gas-phase structure of CCl_3SCN was performed by means of gas electron diffraction (GED). Relevant geometric parameters obtained by GED, solid-state X-ray diffraction (XRD) and computational calculations are listed together in Table 1 for comparison.

A staggered model was used in the analysis of the GED data of CCl_3SCN. The agreements of radial distribution functions as well as the corresponding structural *R* factor are given in Figure 3. The experimental results described above are generally in agreement with the theoretical values (Table 1).

Available information on the gas-phase structures of compounds belonging to the thiocyanate family is scarce. The structure of methyl thiocyanate has been determined by means of rotational spectroscopy and the structure of propargylthiocyanate has been explored by using gas electron diffraction. We have already studied the structure of CH_2ClSCN in the gas phase by using the latter method.[1] By comparing the structures of CH_2ClSCN and CCl_3SCN, it appears that the bond lengths do not differ significantly between the thiocyanates. Moreover, the C1–S2 bond in CCl_3SCN (1.826(2) Å) is very close to that reported for the CH_3SCN species (1.824(2) Å).

2.3. Molecular Structures in the Solid State

The structure of CCl_3SCN in the solid state was determined by X-ray diffraction analysis of a crystal grown in situ in the dif-

Table 1. Experimental and theoretical structural parameters of CCl_3SCN.[a]

	Experimental[b]				Theoretical[c]			
	GED			XRD	B3LYP	MP2	CCSD	CCSD(T)
	r_e	r_g	r_a	r_α	r_e	r_e	r_e	r_e
C1-Cl5	1.765(2)[1]	1.774(2)	1.773(2)	1.763(4)	1.791	1.766	1.770	1.776
C1-Cl6	1.757(2)[1]	1.765(2)	1.764(2)	1.756(5)[f]	1.780	1.758	1.763	1.768
C1-Cl7	1.757(2)	1.765(2)	1.764(2)	1.756(5)[f]	1.780	1.758	1.763	1.768
C1-S2	1.826(2)[1]	1.839(2)	1.838(2)	1.828(1)	1.857	1.829	1.830	1.836
C3-S2	1.691(13)[2]	1.697(13)	1.696(13)	1.696(4)	1.695	1.685	1.698	1.698
C3-N4	1.158(9)[3]	1.163(9)	1.162(9)	1.144(6)	1.156	1.173	1.155	1.164
Cl5-C1-S2	101.4(7)[4]			102.7(2)	102.7	103.1	103.3	103.1
Cl6-C1-S2	112.3(4)[5]			111.6(2)[f]	112.0	111.6	111.7	111.7
Cl5-C1-Cl6	110.6(10)[6]			110.4(2)[f]	110.2	110.4	110.2	110.3
Cl6-C1-Cl7	109.4(20)[d]			110.0(2)	109.6	109.6	109.6	109.6
C1-S2-C3	99.9(17)[7]			98.6(2)	100.6	97.6	98.6	98.4
S2-C3-N4	177.1[e]			177.9(5)	176.3	177.5	177.0	177.1
Cl6-C1-S2-C3	61.9(12)[d]			61.7(3)[f]	61.8	61.5	61.6	61.6

[a] The parameters are given in Å and deg. [b] Threefold standard deviations are in parentheses. Superscript numbers 1, 2, …, 7 indicate groups in which parameters were refined with fixed differences. [c] Dunning triple-zeta cc-pVTZ basis was used in calculations. [d] Dependent parameter. [e] Fixed parameter, see text for details. [f] Average value for the parameters, which are symmetrically equivalent in gas phase.

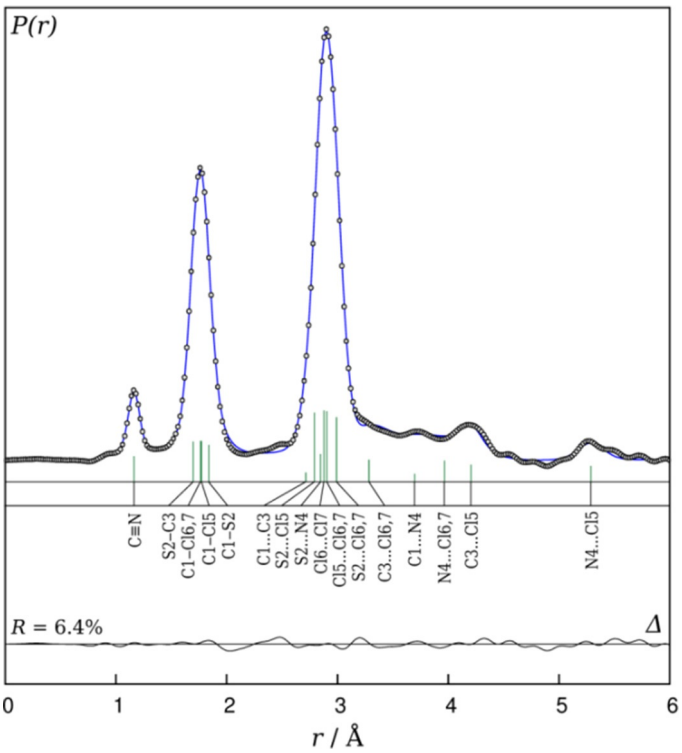

Figure 3. Experimental (circles) and model (line) radial distribution functions of CCl_3SCN. The difference curve is shown below.

fractometer. The compound crystallizes in the monoclinic space group $P2_1/n$, and contains four molecules in the unit cell. As expected, CCl_3SCN in the solid state has a staggered conformation (Figure 4) with a dihedral angle φ(ClC–SC) of 61.7(3)°.

Many thiocyanate compounds have been structurally studied in the crystalline phase by X-ray diffraction. For instance, in 1971, Konnert and Britton reported a crystal structure of methylene dithiocyanate along with its intermolecular interactions and a comparison with other thiocyanates.[7]

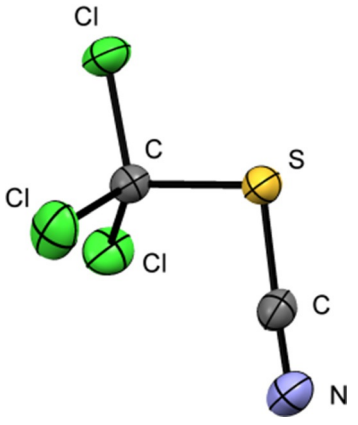

Figure 4. Molecular structure of CCl_3SCN in the crystal as determined by X-ray diffraction at 193 K.

For CCl_3SCN, the C1–S2 bond length in the crystal and in the gas phase are practically the same, even taking into account the different types of geometrical parameters ($r_{\alpha,solid}$ = 1.828(1) Å and $r_{e,gas}$ = 1.826(2) Å, respectively) and resemble the corresponding value found for the *anti*-conformation of CH_2ClSCN in the gas phase (r_e = 1.821(2) Å), but not that obtained for the more stable CH_2ClSCN *gauche*-conformation (1.805(2) Å).[1] This is in excellent agreement with the results described for the gas-phase structure.

2.4. Intermolecular Contacts of CCl_3SCN

The crystal packing and the most significant intermolecular interactions are represented in Figure 5. Five nonbonding inter-

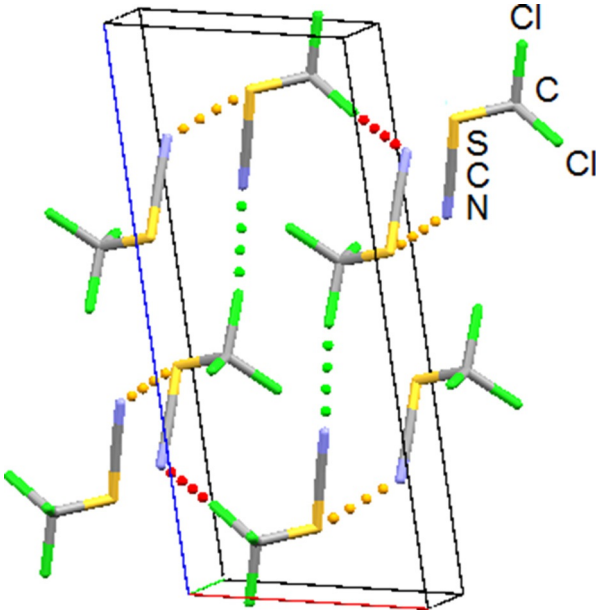

Figure 5. Molecular packing in the crystal and nonbonding intermolecular interactions of CCl_3SCN determined from X-ray diffraction analysis at 193 K.

actions with distances shorter than the sum of the van der Waals radii of the involved atoms were detected (see Table 2). The contact with the shortest distance involves a chlorine atom located in the *anti*-position with respect to the SCN group, and a nitrogen atom from another molecule. This Cl···N interaction, with a distance of 3.09 Å, is considerably shorter than the sum of the corresponding van der Waals radii (3.30 Å). The C(1)–Cl···N angle (171.9°) is consistent with the directionality reported for halogen-type bonding,[8] in which the chlorine atom acts as an electron acceptor along an extension of the C(1)–Cl axis. Figure 5 shows this head (CCl_3) to tail (SCN) interaction represented by green dashed lines.

The sulfur atom in CCl_3SCN participates as an electron acceptor in a chalcogen-type N···S intermolecular interaction, with a C(1)–S···N angle of 158.9°—not too far from the expected 180°. The distance between the two atoms involved in this contact is close to that reported by Konnert and Britton (3.17 Å).[7]

Table 2. Characteristics of nonbonding intermolecular interactions in CCl_3SCN.

Intermolecular contact	Distance [Å]	Angle [degrees]	Sum of van der Waals radii [Å]	Length r_{vdW}[e] [Å]	Contact type proposed
N[a]···Cl-C(1)[b]	3.09	171.9	3.30	−0.21	halogen bond
N[a]···S-C(1)[c]	3.21	158.9	3.35	−0.14	chalcogen bond
N[a]···C3-N[c]	3.22	99.9	3.25	−0.03	–
N[a]···Cl-C(1)[c]	3.24	152.0	3.30	−0.06	–
S[a]···Cl-C(1)[d]	3.54	159.7	3.55	−0.01	–

[a] *x*, *y*, *z*; [b] 1/2+*x*, 1/2−*y*, 1/2+*z*; [c] 3/2−*x*, −1/2+*y*, 1/2−*z*; [d] *x*, 1+*y*, *z*; [e] Intermolecular length minus the sum of the van der Waals radii of the two atoms involved in the contact.

Three other intermolecular contacts with lengths shorter than the sum of the corresponding van der Waals radii are depicted in Table 2. Nevertheless, the shortening of these contacts is not pronounced enough to classify them as halogen or chalcogen interactions. For instance, the intermolecular contact C–Cl···S possibly corresponds to halogen bonding, with a positive electrostatic potential σ-hole along the C(1)–Cl axis directed to the S atom with negative electrostatic potential, but its shortening by 0.01 Å does not allow to assign this with certainty.

The title thiocyanate presents a square-base pyramidal structure around the sulfur atom (Figure 6), which simultaneously acts as an electron acceptor (chalcogen interaction) and as an electron donor (possible halogen interaction).

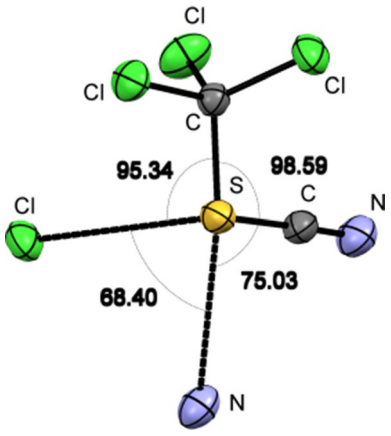

Figure 6. Square-base pyramidal coordination around the sulfur atom in CCl_3SCN.

3. Conclusions

Both crystal and gas-phase structures of CCl_3SCN were determined and compared. They are similar in both phases. Despite the C≡N bonds being similar in the crystal ($r_\alpha = 1.144(6)$ Å) and gas phase ($r_e = 1.158(9)$ Å) according to the standard 3σ criterion, differences $r_e - r_\alpha$ for this C≡N bond were estimated by using the first-order vibrational perturbation theory[9–11] to be 0.014 Å taking into account the different temperatures in GED and XRD experiments. The intermolecular interactions between the CCl_3SCN molecules form a network of halogen and chalcogen interactions, which were detected in the crystal structure.

Experimental Section

Synthesis

The reaction of CCl_3SCl with KCN in diethyl ether was used to prepare trichloromethyl thiocyanate. Several trap-to-trap distillations were performed to purify the sample.[12] The identity and purity of the compound was verified by infrared spectroscopic analysis.

Quantum-Chemical Calculations

The Gaussian 03 package[13] was used to perform DFT[9] and MP2(full)[10] calculations. The nature of the minimum on the potential hypersurface was confirmed according to the harmonic frequencies calculated.

To support the GED structural analyses, analytical harmonic and numeric cubic force fields were calculated at the B3LYP/6-31G(d) and O3LYP/cc-pVTZ levels of theory. The achieved values were subsequently used to calculate mean-square interatomic vibrational amplitudes and corrections to the equilibrium structure by using the SHRINK program.[9–11] Coupled-cluster CCSD and CCSD(T)[14] analytical gradient-powered geometry optimizations were performed by using the Cfour program package.[15] NBO[16] analyses were performed with the NBO package contained in the Gaussian 03 program.

Gas Electron Diffraction

Gas electron diffraction patterns were measured with the improved Balzers Eldigraph KDG2 gas-phase electron diffractometer[17] at Bielefeld University. Table S1 (see the Supporting Information) lists the experimental GED details.

Diffraction patterns were recorded with Fuji BAS-IP MP2 2025 imaging plates, which were subsequently scanned with a calibrated Fuji BAS-1800II scanner. The intensity curves (Figure S1 and S2) were retrieved from the scanned diffraction images by applying a method described earlier.[18] Sector function and electron wavelength were calibrated[19] by using benzene diffraction patterns, recorded along with the substance under investigation. Experimental amplitudes were refined in groups (see Table S2). For this purpose, scale factors (one per group) were used as independent parameters. The ratios between different amplitudes in one group were fixed at the theoretical values. Experimental Cartesian coordinates of CCl_3SCN are depicted in Table S3.

Two sets of theoretical amplitudes and corrections, calculated from B3LYP/6-31G(d) and O3LYP/cc-pVTZ force fields, were tested in the refinements. Those calculated at the B3LYP/6-31G(d) level allowed better agreement with experimental data to be obtained and were used in the final model. The model with staggered orientation of the CCl_3 group with respect to the SCN group was tested. The largest correlations (more than 0.7) were r(S2–C3)/l_1 = 0.82, <(S2–C1–Cl6)/l_1 = −0.78, <(S2–C1–Cl5)/<(S2-C1-Cl6) = −0.72.

Table 3. Details of the X-ray diffraction data.

Chemical formula	CCl_3SCN
M_r	176.5
Unit cell, space group	monoclinic, $P2_1/n$
Temperature [K]	193(1)
a [Å]	6.7972(1)
b [Å]	5.84730(2)
c [Å]	16.1547(2)
β [°]	101.248(1)
V [Å^3]	629.740(16)
Z	4
ρ_{calc} (calculated) [g cm^{-3}]	1.8610
F(000)	320
Crystal color	Colorless
Crystal description	Cylindrical
Wavelength [Å]	0.71073
μ [mm^{-1}]	1.65
Crystal size [mm]	0.3
θ range	2.57-30.54°
Completeness to θ_{max}	81.4%
Index ranges h, k, l	−6/6, −8/8, −22/23
Transmission$_{max/min}$	0.75/0.70
R before/after correction	0.0563/0.0307
Collected reflections	9652
Independent reflections	1569
R(int)	0.019
Data/restraints/parameters	1451/0/65
Goodness of fit in F^2	1.053
$R1$/w$R2$ [observed refl.]	0.0231/0.0551
Observed refl. with	$I > 2\sigma(I)$
$R1$/w$R2$ (complete data)	0.0255/0.0571
Extinction coefficient	0.054(2)
$\rho_{max/min}$ [e Å^{-3}]	0.38/−0.39
CCDC	1020625

X-ray Diffraction

Crystallography measurements (see Table 3) were carried out at Essen-Duisburg University. A four-circle Nicolet R3m/V diffractometer, with a MoKα source ($\lambda = 0.71073$ Å) was used.[20] Crystal structures were resolved by using the Patterson method and refined with SHELXTL-Plus Version SGI IRIS indigo Software.[21] The sample was placed in a 0.2–0.3 mm diameter glass capillary, which was closed at both ends. By using a coupled microscope integrated to the diffractometer, the formation of microcrystals (polycrystalline) was observed upon decreasing the sample temperature. The sample was cooled to approximately 15 K below the melting point and, with a melting-zone-by-zone procedure and subsequent recrystallization caused by heating with an infrared laser focused to a very small area of the sample, a single crystal suitable for an X-ray diffraction experiment grew. A detailed description of this technique is reported elsewhere.[22] CCDC 1020625 contains the supplementary crystallographic data for this paper. These data can be obtained free of charge from The Cambridge Crystallographic Data Centre via www.ccdc.cam.ac.uk/data_request/cif.

Acknowledgements

The authors thank the Deutsche Forschungsgemeinschaft (scholarship of Y.B.M. in Germany and core facility GED@BI, MI477/21-1), the Alexander von Humoldt Siftung (stipend for Y. V. V.), Agencia Nacional de Promoción Científica y Técnica (CNPCYT), Consejo Nacional de Investigaciones Científicas y Técnicas (CONICET), Comisión de Investigaciones de la Provincia de Buenos Aires (CIC), Facultad de Ciencias Exactas, Universidad Nacional de La Plata (UNLP) and Bielefeld University for financial support.

Keywords: chalcogens · conformation analysis · density functional calculations · halogens · solid-state structures

[1] Y. B. Martínez, L. S. Rodríguez Pirani, M. F. Erben, C. G. Reuter, Y. V. Vishnevskiy, H. G. Stammler, N. W. Mitzel, C. O. Della Védova, *Phys. Chem. Chem. Phys.* **2015**, *17*, 15805 – 15812.
[2] J. F. Olin, G. I. Mich, U.S. Patent 278, 955, Mar 27, **1952**.
[3] G. E Lukes, U.S. Patent 3,361,621, May 31, **1963**.
[4] S. E. Ulic, F. Di Napoli, A. Hermann, H. G. Mack, C. O. Della Védova, *J. Raman Spectorosc.* **2000**, *31*, 909 – 913.
[5] J. R. Duarte, G. L. Sosa, *J. Mol. Model.* **2013**, *19*, 2035 – 2041.
[6] U. Adhikari, S. Scheiner, *J. Phys. Chem. A* **2012**, *116*, 3487 – 3497.
[7] J. H. Konnert, D. Britton, *Acta Crystallogr. Sect. B* **1971**, *27*, 781 – 786.
[8] a) R. G. Gonnade, M. S. Shashidhar, M. M. J. Bhadbhade, *Ind. Institute Sci.* **2007**, *87*, 149 – 165; b) P. Politzer, J. S. Murray, *ChemPhysChem* **2013**, *14*, 278 – 294; c) J. S. Murray, P. Politzer, T. Clark, *Phys. Chem. Chem. Phys.* **2013**, *15*, 11178 – 11189.
[9] R. G. Parr, W. Yang, *Density-Functional Theory of Atoms and Molecules*, Oxford University Press, New York, **1989**.
[10] C. Møller, M. S. Plesset, *Phys. Rev.* **1934**, *46*, 618 – 622.
[11] V. A. Sipachev, *J. Mol. Struct.* **2004**, *693*, 235 – 240.
[12] H. Brintzinger, K. Pfannstiel, H. Koddebusch, K. E. Kling, *Chem. Ber.* **1950**, *83*, 87 – 90.
[13] Gaussian 03, Revision B.01, M. J. Frisch, G. W. Trucks, H. B. Schlegel, G. E. Scuseria, M. A. Robb, J. R. Cheeseman, J. A. Montgomery, Jr., T. Vreven, K. N. Kudin, J. C. Burant, J. M. Millam, S. S. Iyengar, J. Tomasi, V. Barone, B. Mennucci, M. Cossi, G. Scalmani, N. Rega, G. A. Petersson, H. Nakatsuji, M. Hada, M. Ehara, K. Toyota, R. Fukuda, J. Hasegawa, M. Ishida, T. Nakajima, Y. Honda, O. Kitao, H. Nakai, M. Klene, X. Li, J. E. Knox, H. P. Hratchian, J. B. Cross, C. Adamo, J. Jaramillo, R. Gomperts, R. E. Stratmann, O. Yazyev, A. J. Austin, R. Cammi, C. Pomelli, J. W. Ochterski, P. Y.Ayala, K. Morokuma, G. A. Voth, P. Salvador, J. J. Dannenberg, V. G. Zakr-zewski, S. Dapprich, A. D. Daniels, M. C. Strain, O. Farkas, D. K. Malick, A. D. Rabuck, K. Raghavachari, J. B. Foresman, J. V. Ortiz, Q. Cui, A. G. Baboul, S. Clifford, J. Cioslowski, B. B. Stefanov, G. Liu, A. Liashenko, P. Piskorz, I. Komaromi, R. L. Martin, D. J. Fox, T. Keith, M. A. Al-Laham, C. Y. Peng, A. Nanayakkara, M. Challacombe, P. M. W. Gill, B. Johnson, W. Chen, M. W. Wong, C. Gonzalez, J. A. Pople, Gaussian, Inc., Pittsburgh, PA, **2003**.
[14] K. Raghavachari, G. W. Trucks, J. A. Pople, M. A. Head-Gordon, *Chem. Phys. Lett.* **1989**, *157*, 479 – 483.
[15] M. E. Harding, T. Metzroth, J. Gauss, A. A. Auer, *J. Chem. Theory Comput.* **2008**, *4*, 64 – 74.
[16] J. P. Foster, F. Weinhold, *J. Am. Chem. Soc.* **1980**, *102*, 7211 – 7218.
[17] a) R. J. F. Berger, M. Hoffmann, S. A. Hayes, N. W. Mitzel, *Z. Naturforsch. B* **2009**, *64*, 1259 – 1268; b) C. G. Reuter, Y. V. Vishnevskiy, S. Blomeyer, N. W. Mitzel, *Z. Naturforsch. B* **2016**, *71*, 1 – 13.
[18] Y. V. Vishnevskiy, *J. Mol. Struct.* **2007**, *833*, 30 – 41.
[19] Y. V. Vishnevskiy, *J. Mol. Struct.* **2007**, *871*, 24 – 32.
[20] R. Boese, M. Nussbaumer, *Correlations, Transformations and Interactions in Organic Crystal Chemistry, Vol. 7* (Eds.: D. W. Jones, A. Katrusiak), IUCr Crystallographic Symposia, Oxford, **1994**, pp. 20 – 37.
[21] G. M. Sheldrick, *Acta Crystallogr. Sect. A* **2008**, *64*, 112 – 122.
[22] D. Brodalla, D. Mootz, R. Boese, W. Osswald, *J. Appl. Crystallogr.* **1985**, *18*, 316 – 319.

Manuscript received: January 15, 2016
Accepted Article published: February 11, 2016
Final Article published: March 10, 2016